

# HIV-1 Tat Protein Increases Microglial Outward $K^+$ Current and Resultant Neurotoxic Activity

Jianuo Liu<sup>1\*</sup>, Peng Xu<sup>1</sup>, Cory Collins<sup>1</sup>, Han Liu<sup>1</sup>, Jingdong Zhang<sup>1</sup>, James P. Keblesh<sup>1</sup>, Huangui Xiong<sup>1,2\*</sup>

**1** Neurophysiology Laboratory, Department of Pharmacology and Experimental Neuroscience, University of Nebraska Medical Center, Omaha, Nebraska, United States of America, **2** Department of Pathology and Microbiology, University of Nebraska Medical Center, Omaha, Nebraska, United States of America

## Abstract

Microglia plays a crucial role in the pathogenesis of HIV-1-associated neurocognitive disorders. Increasing evidence indicates the voltage-gated potassium ( $K_v$ ) channels are involved in the regulation of microglia function, prompting us to hypothesize  $K_v$  channels may also be involved in microglia-mediated neurotoxic activity in HIV-1-infected brain. To test this hypothesis, we investigated the involvement of  $K_v$  channels in the response of microglia to HIV-1 Tat protein. Treatment of rat microglia with HIV-1 Tat protein (200 ng/ml) resulted in pro-inflammatory microglial activation, as indicated by increases in TNF- $\alpha$ , IL-1 $\beta$ , reactive oxygen species, and nitric oxide, which were accompanied by enhanced outward  $K^+$  current and  $K_v1.3$  channel expression. Suppression of microglial  $K_v1.3$  channel activity, either with  $K_v1.3$  channel blockers Margatoxin, 5-(4-Phenoxybutoxy)psoralen, or broad-spectrum  $K^+$  channel blocker 4-Aminopyridine, or by knockdown of  $K_v1.3$  expression via transfection of microglia with  $K_v1.3$  siRNA, was found to abrogate the neurotoxic activity of microglia resulting from HIV-1 Tat exposure. Furthermore, HIV-1 Tat-induced neuronal apoptosis was attenuated with the application of supernatant collected from  $K^+$  channel blocker-treated microglia. Lastly, the intracellular signaling pathways associated with  $K_v1.3$  were investigated and enhancement of microglial  $K_v1.3$  was found to correspond with an increase in Erk1/2 mitogen-activated protein kinase activation. These data suggest targeting microglial  $K_v1.3$  channels may be a potential new avenue of therapy for inflammation-mediated neurological disorders.

**Citation:** Liu J, Xu P, Collins C, Liu H, Zhang J, et al. (2013) HIV-1 Tat Protein Increases Microglial Outward  $K^+$  Current and Resultant Neurotoxic Activity. PLoS ONE 8(5): e64904. doi:10.1371/journal.pone.0064904

**Editor:** Michelle L. Block, Virginia Commonwealth University, United States of America

**Received:** March 21, 2013; **Accepted:** April 19, 2013; **Published:** May 30, 2013

**Copyright:** © 2013 Liu et al. This is an open-access article distributed under the terms of the Creative Commons Attribution License, which permits unrestricted use, distribution, and reproduction in any medium, provided the original author and source are credited.

**Funding:** This work was supported by a research grant from National Institutes of Health (NIH): R01NS077873 to HX. The funders had no role in study design, data collection and analysis, decision to publish, or preparation of the manuscript.

**Competing Interests:** The authors have declared that no competing interests exist.

\* E-mail: jnliu@unmc.edu (JL); hxiong@unmc.edu (HX)

## Introduction

Individuals infected with human immunodeficiency virus type 1 (HIV-1) often suffer from neurocognitive impairments which are referred to as HIV-1-associated neurocognitive disorders (HAND) [1,2]. The severity of HAND varies, ranging from asymptomatic neurocognitive impairment to its severest form: HIV-1-associated dementia [2]. Despite the widespread use of potent antiretroviral therapy (ART), the incidence of HAND has not been fully prevented and its prevalence remains high ranging from 39% to 52% in varied settings [3,4,5]. Although the persistence of HAND is multifactorial, the paucity of effective therapeutic modalities in the control of brain macrophage and microglia activation and resultant production of neurotoxins, a striking pathological feature in HIV-1-infected brain, plays an important role as pathogenesis and severity of HAND is highly correlated with activated brain macrophages and microglia but not the presence and amount of virus in the brain [6,7]. It is well known that the activated microglia secrete a number of neurotoxins including, but not limited to, pro-inflammatory cytokines, and excitatory amino acids, reactive oxygen species (ROS), nitric oxygen (NO), which can result in neuronal injury and consequent neurocognitive impairments [8,9,10]. As such, studies on elucidation of the mechanisms by which HIV-1 triggers microglial neurotoxicity and identification of specific target(s) to control microglia activation are imperative.

Voltage-gated potassium ( $K_v$ ) channels have recently gained much attention as the potential targets for therapy of neurological disorders [11,12]. Electrophysiological studies of microglia in culture and tissue slices have demonstrated that microglia express several types of  $K_v$  channels including inward rectifier  $K_{ir}2.1$  and outward rectifiers  $K_v1.5$  and  $K_v1.3$ . Exposure to a variety of activating stimuli produces a characteristic pattern of up-regulation of  $K_v1.3$  [13,14,15,16]. Whereas the expression of  $K_{ir}2.1$  channels are often found in resting microglia [17,18], the expression of  $K_v1.5$  and  $K_v1.3$ , especially the latter, appear to be associated with microglia activation and neurotoxin production [15,19,20,21]. Indeed, studies have shown that activation of microglia results in neuronal injury through a process requiring  $K_v1.3$  activity in microglia. Studies have also shown that blocking microglia  $K_v1.3$  or decrease of  $K_v1.3$  expression inhibits microglia-induced neurotoxicity [22,23]. We hypothesize that HIV-1 brain infection triggers microglia neurotoxic activity by increasing  $K_v1.3$  activity, resulting in microglia activation and consequent neuronal injury. To test this hypothesis, we studied involvement of  $K_v1.3$  in HIV-1 Tat protein-induced microglia activation and resultant neurotoxic activity in primary microglia culture prepared from Sprague-Dawley rats. Our results demonstrated that HIV-1 Tat increases microglia production of neurotoxins and resultant neurotoxicity through enhancements of  $K_v1.3$  protein expression and outward  $K^+$  currents, which can be blocked by pretreatment

of microglia with specific K<sub>v</sub> channel blockers Margatoxin (MgTx) or 5-(4-Phenoxybutoxy)psoralen (PAP), or by transfection of microglia with K<sub>v</sub>1.3 siRNA, suggesting an involvement of K<sub>v</sub>1.3 in microglia-mediated neurotoxic activity. The enhancements of K<sub>v</sub>1.3 channel activity and microglia neurotoxicity resulting from HIV-1 Tat protein exposure are dependent on the Erk1/2 MAPK signal pathway. Here we present evidence for the reduction of neurotoxic secretions from microglia and associated neuronal injury by modulation of K<sup>+</sup> channel activity as a potential new treatment approach deserving further investigation.

## Materials and Methods

### Animals

Sprague-Dawley rats were purchased from Charles River Laboratories (Wilmington, MA) and maintained under ethical guidelines for care of laboratory animals at the University of Nebraska Medical Center. All animal-use procedures were reviewed and approved by the Institutional Animal Care and Use Committee (IACUC) of University of Nebraska Medical Center (IACUC # 00-062-07).

### Primary microglia and neuron cultures

Microglia were derived from the cerebral cortices of 0–1 day old neonatal Sprague Dawley rats as described previously [24]. Cortical tissues were dissected in cold Hanks' Balanced Salt Solution (HBSS; Madiatech, Inc. Manassas, VA) and digested in a solution consisting of 0.25% trypsin and 200 Kunitz DNase (Sigma, St. Louis, MO) at 37°C for 30 min. Tissues were then suspended in cold HBSS and filtered using 100 µm and 40 µm cellular strainers (BD Bioscience, Durham, NC). Isolated cells (30×10<sup>6</sup>) were plated into T75 cm<sup>2</sup> flasks in a high-glucose Dulbecco's modified Eagle's medium (DMEM) supplemented with 10% fetal bovine serum (FBS), 2 mM L-glutamine, 1% penicillin/streptomycin, and 1 µg/ml macrophage colony-stimulating factor (Life Technologies, Grand Island, NY). After 10 day's culture, flasks were shaken gently to detach cells, which were plated based on experimental requirements in either 35 mm<sup>2</sup> culture dishes (2.5×10<sup>6</sup> cells/dish), 60 mm<sup>2</sup> culture dishes (7.5×10<sup>6</sup> cells/dish), 12-well plates (1×10<sup>6</sup>/well), or 96-well plates (0.4×10<sup>6</sup>/well) and incubated at 37°C. After 30 min, suspended glial cells were removed by aspiration of culture supernatant and fresh culture media was applied. The resulting cultures were stained with OX-42 antibody (Serotec, Oxford, UK), a microglial CR3/CD11b receptor marker, and determined to consist of 98–100% microglia.

Primary cortical neurons were prepared from 18-day old Sprague Dawley embryonic rats (Charles River Laboratories). Dissected cortices were digested with 0.25% trypsin and DNase (200 Kunitz) in 37°C for 15 min, then filtered through 100 and 40 µm pore cellular strainers. Isolates were seeded in pre-coated poly-D-lysine plates at a density of 0.05×10<sup>6</sup> cells/well in 96-well plates, 0.15×10<sup>6</sup> cells/well in 24-well plates, or 1.0×10<sup>6</sup> cells/well in 6 well-plates. Neuronal cultures were maintained at 37°C for 10 days in neurobasal medium (Gibco by Life Technologies) supplemented with 2% B27, 1% penicillin/streptomycin and 0.5 mM L-glutamine (Invitrogen by Life Technologies). The purity of neuronal cells was determined to be >90% by staining with microtubule-associated protein-2 antibody (MAP-2: 1:1000, Chemicon International, Inc. Temecula, California).

### Electrophysiology

Whole-cell outward K<sup>+</sup> currents were recorded from primary rat microglia cultures at room temperature. Microglia were perfused with artificial cerebrospinal fluid (ACSF) contained (in

mM) NaCl 150, KCl 4.5, CaCl<sub>2</sub> 2, MgCl<sub>2</sub> 1, HEPES 5, and glucose 11. The ACSF was continuously oxygenated with 95% O<sub>2</sub> and 5% CO<sub>2</sub> with a pH of 7.4 and an osmolarity of 310 mOsm. Patch-clamp electrodes were made from borosilicate glass capillaries (WPI, Sarasota, FL) with a resistance of 4–6 MΩ when filled with pipette solution contained (in mM) KCl 150, MgCl<sub>2</sub> 1, CaCl<sub>2</sub> 1, EGTA 11, and HEPES 10; adjusted to a pH of 7.3 with KOH. Voltage-dependent currents were evoked by voltage steps (600 ms in duration) with the first step from the holding potential of −70 mV to −170 mV and then stepped to +50 mV with a 20 mV increments [13]. The seal resistance was 1–10 GΩ. Junction potentials were corrected and the cell capacitance was compensated (~70%) in most cells. Current signals were amplified with an Axopatch 200B amplifier (Molecular Devices, Sunnyvale, CA). The current traces were displayed and recorded on a Dell computer using a pClamp 10.1 data acquisition/analysis system. K<sup>+</sup> current density (pA/pF) was calculated by dividing the peak current amplitude generated at a given voltage step by the cell capacitance.

### Measurement of reactive oxygen species (ROS) and Nitric oxide (NO) production

Intracellular ROS were measured by fluorometric assay using 2', 7'-dichlorofluorescein diacetate (DCFH-DA, Sigma, St. Louis, MO), a well-established compound for detecting and quantifying intracellular ROS production. Microglia were first treated for 30 minutes with a K<sub>v</sub>1.3 channel blocker, either 5 nM MgTx, 10 nM PAP, or 1 mM 4-AP (all purchased from Sigma-Aldrich Co, LLC, St. Louis, MO), followed by treatment with either 200 ng/ml of HIV-1 Tat<sub>1-72</sub> protein (Tat) or heat inactivated-Tat<sub>1-72</sub> (HI Tat) (purchased from University of Kentucky). After 24 hr, microglia were exposed to 20 µM DCFH-DA for 30 min. Cells were then washed twice in PBS and the fluorescence immediately measured in a plate reader at an excitation wavelength of 485 nm and an emission wavelength of 520 nm.

NO production was estimated by measuring the concentration of nitrite using the Griess Reagent System according to the manufacturer instruction (Promega, Madison, WI). 50 µl aliquots of supernatant were collected from cultures of pre-treated microglia, mixed with equal volume of Sulfanilamide Solution for 10 min, combined with 50 µl of NED solution, and incubated for 30 min at room temperature. The optical density was then measured at 520 nm and 540 nm using an ELISA plate reader. All experiments were repeated at least three times.

### Cytokine assay

Cytokines IL-1β and TNF-α in pre-treated microglia supernatants were quantified using specific enzyme-linked immunosorbent assay (ELISA) kits (R&D Systems) in accordance with manufacturer protocol.

### TUNEL staining and MTT assay

Neuronal apoptosis was evaluated using a Fluorescein *In Situ* Cell Death Detection Kit (Roche Applied Science, Indianapolis, IN). In brief, neurons growing on poly-D-lysine-coated coverslips (0.15×10<sup>6</sup> cells/well in a 24-well plate) were exposed to supernatants collected from pre-treated microglia at 1:5 dilution for 24 hr. Neurons were then fixed with 4% paraformaldehyde (PFA) and permeabilized with 0.1% Triton X-100. Neurons were subsequently incubated in the TUNEL reaction mixture for 1 hr at 37°C and then mounted using ProLong Gold antifade reagent with 4',6'-diamidino-2-phenylindol (DAPI) counterstain (Molecular Probes, Eugene, OR). Cells were visualized using the 40× oil-

immersion objective of a Zeiss LSM 510 META NLO microscope (Zeiss MicroImaging, Inc., Thornwood, NY). The percentage of apoptotic neurons was determined based on TUNEL-positive cells normalized to DAPI-stained nuclei.

Cell viability was assessed by MTT assay. Pre-treated neurons were exposed to fresh neurobasal medium containing 500 µg/ml 3-(4,5-dimethylthiazol-2-yl)-2,5-diphenyl tetrazolium bromide (MTT) for 3 hr. The MTT solution was then replaced with 300 µl of dimethyl sphingosine (DMSO; Sigma-Aldrich) for cell lysis and the optical density (OD) was measured at 560 nm.

### Immunocytochemistry

Microglia were seeded on coverslips at a density of  $1.0 \times 10^6$ /well in 12-well plates, treated for 30 min with 5 nM MgTx, 10 nM PAP, or 1 mM 4-AP, and incubated with Tat (200 ng/ml). After 24 hr, cells were washed, fixed with 4% PFA for 30 min, and incubated with 10% normal goat serum blocking solution for 30 min. Primary antibodies (Ab) anti-CD11b Ab (CD11b; 1:500; abcam, Cambridge, MA) and anti-K<sub>v</sub>1.3 (KCNA3 1:100, Alomone Lab Ltd, Jerusalem Israel) were then applied to coverslips for 3 hr at RT. Cells were subsequently incubated for 1 hr with Alexa Fluor 488 and Alexa Fluor 594-conjugated secondary Abs (1:1000, Molecular Probes, Invitrogen by Life Technologies). After washing, cells were mounted using ProLong Gold antifade reagent with DAPI counterstain (Molecular Probes). Images were obtained using the 40× oil-immersion objective of a Zeiss LSM 510 META NLO microscope. A minimum of 5 images were taken from each slide.

### Immunohistochemistry

Brain hippocampal tissues were dissected out from 20–30 d old Sprague Dawley rats (Charles River Laboratories), cut into slices at 400 µm in thickness, and placed on a 100 µm pore cellular strainer in a 6-well plate. The hippocampal slices were then treated for 30 min with MgTx (5 nM), PAP (10 nM), or 4-AP (1 mM) and subsequently incubated with 200 ng/ml of Tat. After 24 hr, hippocampal slices were fixed in 4% PFA for another 24 hr, immersed in 30% sucrose for 48 hr, embedded in optimal cutting temperature (OCT) media, and cryosectioned to a thickness of 10 µm. Hippocampal sections were then immunostained with either anti-Iba1 Ab (1:500, WAKO Chemicals USA, Inc. Richmond, VA), K<sub>v</sub>1.3 Ab (1:200, Santa Cruz biotechnology, Inc, CA), or TUNEL stain and visualized using the 40× oil-immersion objective of a Zeiss LSM 510 META NLO microscope. A minimum of 5 images were taken from each slides.

### Western blot analysis

Membrane proteins were prepared using a Membrane Protein Extraction Kit (BioVision, Mountain View, CA, USA) according to manufacturer instruction, while total proteins were isolated using a RIPA buffer (Bio-Rad, Hercules, CA). Well volumes of 20 µg for membrane proteins and 30 µg for total proteins were separated by electrophoresis using 4–15% Mini-PROTEAN TGX precast gel and transferred to nitrocellulose polyvinylidene difluoride (PVDF) membranes. PVDF membranes were then blocked with 5% dry milk in Tris-Buffered Saline (TBS) (all products from Bio-Rad Laboratories, Hercules, CA) and probed overnight at 4°C with either rabbit polyclonal K<sub>v</sub>1.3 (1:100; Alomone Lab, Israel), phospho-p44/42 MAPK (pERK1/2), total p44/42 MAPK (ERK1/2) (1:1000; Cell Signaling Technology, Danvers, MA), or anti-mouse β-actin monoclonal antibody (1:10,000, Sigma-Aldrich) primary Abs. Membranes were next washed (4×10 min) in TBS with 0.2% Tween (TBS-T) and incubated for 1 hr at RT with either horseradish peroxidase

(HRP)-conjugated anti-rabbit or anti-mouse secondary antibody (1:10,000, Jackson ImmunoResearch Laboratories, West Grove, PA). Labeled proteins were visualized by Pierce ECL Western Blotting Substrate (Thermo Scientific, Rockford, IL). Band densities of p-pErk1/2 were normalized to total ERK1/2 in each sample.

### Reverse transcription (RT)-PCR

Total RNA was isolated from microglia using TRIzol Reagent (Invitrogen, Carlsbad, CA), purified by RNeasy Mini Kit (QIAGEN, Inc., Valencia, CA), and reverse transcribed at 65°C for 50 min according to SuperScript III reverse transcriptase (Invitrogen) protocol. PCR amplification with Platinum PCR SuperMix (Invitrogen) then included 2 min incubation at 94°C followed by 30 cycles consisting of a 30 s denaturing phase at 94°C, a 30 s annealing phase at 55°C, a 1 min extension phase at 72°C, and a final extension phase of 10 min at 72°C. Densitometry analysis of DNA products was performed using Northern Eclipse 6.0 software (Bio-Rad) and results normalized to β-actin internal controls. PCR primers used were as follows: forward K<sub>v</sub>1.3 primer was GTA CTT CGA CCC GCT CCG CAA TGA; reverse K<sub>v</sub>1.3 primer was GGG CAA GCA AAG AAT CGC ACC AG; forward β-Actin primer was GTG GGG CGC CCC AGG CAC CA; reverse β-Actin primer was CTT CCT TAA TGT CAC GCA CGA TTT C.

### siRNA transfection

Pre-designed ON-TARGETplus SMARTpool siRNA against rat KCNA3 (K<sub>v</sub>1.3, NM-019270) mRNA was purchased from Dharmacon, Inc. (Chicago, IL). Microglia plated to  $2 \times 10^6$  cells/well in 6-well plates were transfected with 100 µl of 2 µM siRNA for 48 or 72 hr in the presence of Dharma FECT Transfection Reagent (Dharmacon, Inc) according to the manufacturer instruction. A non-specific ON-TARGETplus GAPD Control Pool siRNA (rat) (Dharmacon, Inc) was also similarly transfected at the same concentration as the control. Transfected microglia were then incubated for 24 hr with or without Tat (200 ng/ml), after which the supernatant was collected (for conditioned media) and the cells were harvested (for preparation of RNA and protein).

### Statistical Analysis

Experimental data are expressed as mean ± S.D. unless otherwise indicated. Statistical analyses were performed by Student *t* tests. A minimum *p* value of 0.05 was estimated as the significance level for all tests.

## Results

### HIV-1 Tat exposure induces K<sub>v</sub>1.3 currents in microglia

HIV-1 pathogenesis involves the release of soluble viral proteins such as gp120, Tat, and Nef. In previous studies, we demonstrated HIV-1 gp120 IIIB enhanced whole-cell outward K<sup>+</sup> current in cultured rat microglia through K<sub>v</sub>1.3 channels [24,25]. Here we propose HIV-1 Tat protein may alter microglia channel profiles in a similar manner. To test our hypothesis, we first examined the effect of HIV-1 Tat protein on the electrophysiological properties of microglia. Although sera levels of HIV-1 Tat have been reported to range from 1–40 ng/ml in HIV-1 positive individuals [26,27], localized concentrations are reasoned to be higher and nM concentrations are commonly used *in vitro* to elicit the effects of Tat exposure [28,29]. In our study, purified rat microglia were pretreated with HIV-1 Tat protein at 20–1000 ng/ml for 24 hr before recording. Electrophysiological recordings were performed using a conventional whole-cell recording under voltage clamp



configuration. The average inward K<sup>+</sup> current ( $I_{in}$ ) and outward K<sup>+</sup> current ( $I_{out}$ ) densities (pA/pF) were calculated by dividing the K<sup>+</sup> current amplitude by the membrane capacitance. At hyperpolarizing potentials, both untreated and Tat treated microglia displayed an  $I_{in}$  (Fig. 1A). The  $I_{in}$  density in untreated microglia ( $-8.96 \pm 3.76$  pA/pF;  $n = 32$ ) was only minimally affected by exposure to either 20 ng/ml Tat ( $-8.14 \pm 3.61$  pA/pF;  $n = 25$ ), 200 ng/ml Tat ( $-15.5 \pm 7.36$  pA/pF;  $n = 27$ ), or 1000 ng/ml Tat ( $-12.9 \pm 7.21$  pA/pF;  $n = 24$ ). With depolarizing pulses however, Tat treated microglia responded with a substantial  $I_{out}$  (Fig. 1A). In fact, the  $I_{out}$  density in microglia pretreated with 20 ng/ml Tat ( $22.69 \pm 7.46$  pA/pF;  $n = 25$ ) was over fourfold greater than in untreated microglia ( $5.09 \pm 2.84$  pA/pF;  $n = 32$ ). Furthermore, the  $I_{out}$  densities in microglia exposed to 200 ng/ml Tat ( $30.7 \pm 16.29$  pA/pF;  $n = 27$ ) and 1000 ng/ml Tat ( $31.86 \pm 14.69$  pA/pF;  $n = 24$ ) demonstrate this effect to be dose-dependent (Fig. 1C). To confirm these observations were due specifically to Tat protein function, we disrupted its tertiary structure with heat (75°C for 5 hr) prior to incubation with microglia. Similarly to untreated cells, microglia treated with 200 ng/ml heat-inactivated Tat protein (HI Tat,  $n = 9$ ) exhibited hyperpolarization-evoked  $I_{in}$  currents and lacked significant  $I_{out}$  current in response to depolarizing pulses (Fig. 1B). Next, to determine whether the Tat-induced  $I_{out}$  currents were conducted via K<sub>v</sub>1.3 channels, Tat-treated microglia were perfused with ACSF contained specific K<sub>v</sub>1.3 blockers PAP (10 nM), MgTx (5 nM), or a broad spectrum K<sub>v</sub> channel blocker 4-AP (1 mM), and the  $I_{out}$  was significantly reduced by  $52.1 \pm 14.72\%$  ( $n = 8$ ),  $87.26 \pm 7.79\%$  ( $n = 8$ ) or  $89.81 \pm 3.09\%$  ( $n = 7$ ) (Fig. 1D & 1E). Taken together, these findings strongly suggest HIV-1 Tat exposure induces outward K<sup>+</sup> currents in microglia through K<sub>v</sub>1.3 channels.

### HIV-1 Tat upregulates K<sub>v</sub> 1.3 expression in rat microglia

K<sub>v</sub> channel activity can be altered by numerous factors, including by membrane potential, redox potential, transcription, translation, posttranslational modification, or via direct interaction with organic molecules or peptides. To better determine the mechanism through which Tat induces K<sub>v</sub>1.3 currents in rat microglia, K<sub>v</sub>1.3 mRNA and protein levels were ascertained by RT-PCR and western blot. RT-PCR performed after 24 hr incubation of rat microglia with 200 ng/ml Tat protein showed marked elevation in K<sub>v</sub>1.3 mRNA expression (Fig. 2A), with K<sub>v</sub>1.3 mRNA density in Tat-treated cells ( $1.32 \pm 0.10$ ) measuring 1.8 times greater than in untreated microglia ( $0.74 \pm 0.23$ ). As a negative control, the K<sub>v</sub>1.3 mRNA density was measured in microglia treated with 200 ng/ml heat-inactivated Tat protein and found to be essentially unchanged ( $0.81 \pm 0.13$ ) (Fig. 2A). Consistent with these effects, treatment of microglia with 200 ng/ml Tat for 24 hr led to a nearly threefold increase in K<sub>v</sub>1.3 protein levels (Fig. 2B), which was further confirmed and visualized by immunocytochemical labeling (Fig. 2C). These findings clearly indicate Tat protein exposure upregulates the expression of K<sub>v</sub>1.3 channels in rat microglia.

### Involvement of K<sub>v</sub>1.3 in Tat-induced microglia-mediated neurotoxicity

Having established Tat protein exposure increases K<sub>v</sub>1.3 expression and current density in microglia, we next sought to determine if this change in channel profile contributes to the neurotoxicity of HIV-1 Tat-activated microglia. Microglial supernatants were first collected after 24 hr treatment with either HIV-1 Tat protein (at doses of 0, 20, 200, and 1000 ng/ml) or heat-inactivated Tat (200 ng/ml). Rat cortical neurons growing on

poly-D-lysine-coated coverslips in 24-well plates were then subjected to these supernatants (1:5 dilution) for an additional 24 hr and neuronal viability was assessed by MTT assay. As shown in Figure 3C, neuronal cell viability was found to be essentially unaffected at doses of 0 ng/ml (100%) and 20 ng/ml ( $97.02 \pm 9.38\%$ ), however was progressively and significantly reduced as the microglial supernatant Tat treatment dose was increased to 200 ng/ml ( $70.19 \pm 3.33\%$ ;  $p < .01$ ) and 1000 ng/ml ( $58.45 \pm 4.65\%$ ;  $p < .01$ ). Neuronal viability was further unaffected by incubation with supernatant collected from microglia treated with heat-inactivated Tat protein (HI Tat,  $98.4 \pm 4.48\%$ ), demonstrating the dose-dependent reductions in viability to be specific to functional Tat protein.

Next, the role of K<sub>v</sub> channels in Tat-activated microglial neurotoxicity was investigated using a similar experimental design and examining the effect of K<sub>v</sub> channel blocker pretreatment on neuronal health. Microglia were first pretreated with either 5 nM MgTx, 10 nM PAP, or 1 mM 4-AP for 30 min. Based on the capacity to substantially reduce neuronal viability, a dose of 200 ng/ml Tat protein was applied and cultures incubated for 24 hr. Microglia supernatants were then collected and added to cultured rat cortical neurons at a dilution ratio of 1:5. After 24 hr, neuronal viability and neuronal apoptosis were assessed by MTT assay and TUNEL staining, respectively. As noted previously, cell viability was shown by MTT assay to be decreased in neuronal cultures exposed to Tat-treated microglial supernatant ( $70.19 \pm 3.33\%$ ), an effect which was significantly attenuated ( $p < .01$ ) by the pretreatment of microglia with MgTx ( $85.46 \pm 1.00\%$ ), PAP ( $82.95 \pm 0.54\%$ ), or 4-AP ( $92.83 \pm 4.66\%$ ) (Fig. 3C). The complementary study of neuronal apoptosis revealed similar findings, with the percentage of apoptotic neurons greatly increasing ( $p < .001$ ) with application of Tat protein ( $30.68 \pm 4.3\%$ ) compared to control ( $5.6 \pm 1.3\%$ ) (Fig. 3A & 3B). Again, this result was largely reversed ( $p < .01$ ) when microglial cultures were treated with MgTx ( $9.56 \pm 2.78\%$ ), PAP ( $11.72 \pm 2.42\%$ ), or 4-AP ( $7.29 \pm 3.84\%$ ) prior to the application of Tat protein (Fig. 3A & 3B). The recovery of neuronal viability and attenuation of neuronal apoptosis by K<sub>v</sub> channel blockade, including the use of K<sub>v</sub>1.3 specific inhibitors, suggests that K<sub>v</sub>1.3 channel activity greatly impacts Tat-induced microglia-mediated neurotoxicity.

### K<sub>v</sub>1.3 channel blockade decreases neurotoxic secretions by Tat-activated microglia

The production and release of bioactive molecules by activated microglia is believed to be the principal pathway in HAND associated neuropathology. To better clarify the functional role of K<sub>v</sub>1.3 channels in this process, we next examined the capacity for Tat exposure to induce the secretion of proinflammatory cytokines such as TNF- $\alpha$  and IL-1 $\beta$ , in the presence and absence of K<sub>v</sub> channel blockers. For this experiment, purified microglia were first pre-treated for 30 min with a K<sub>v</sub> channel blocker, either MgTx (5 nM), PAP (10 nM), or 4-AP (1 mM), and then incubated with 200 ng/ml Tat protein for 24 hr. Subsequent cytokine assays revealed marked increases ( $p < .001$ ) in levels of TNF- $\alpha$  ( $2.28 \pm 0.07$  ng/ml) and IL-1 $\beta$  ( $4.10 \pm 0.68$  ng/ml) in the supernatants of Tat-treated microglia compared to the nearly undetectable levels in untreated controls (Fig. 4A & 4B). Further, this Tat-induced production of cytokines was significantly inhibited ( $p < .01$ ) in cultures pretreated with K<sub>v</sub> channel blockers MgTx, PAP, or 4-AP. In addition to measuring cytokines, we used a similar experimental design to measure other neurotoxic microglial products including NO and ROS. The level of NO in supernatants from Tat-treated microglia was ( $23.65 \pm 0.60$  nM)

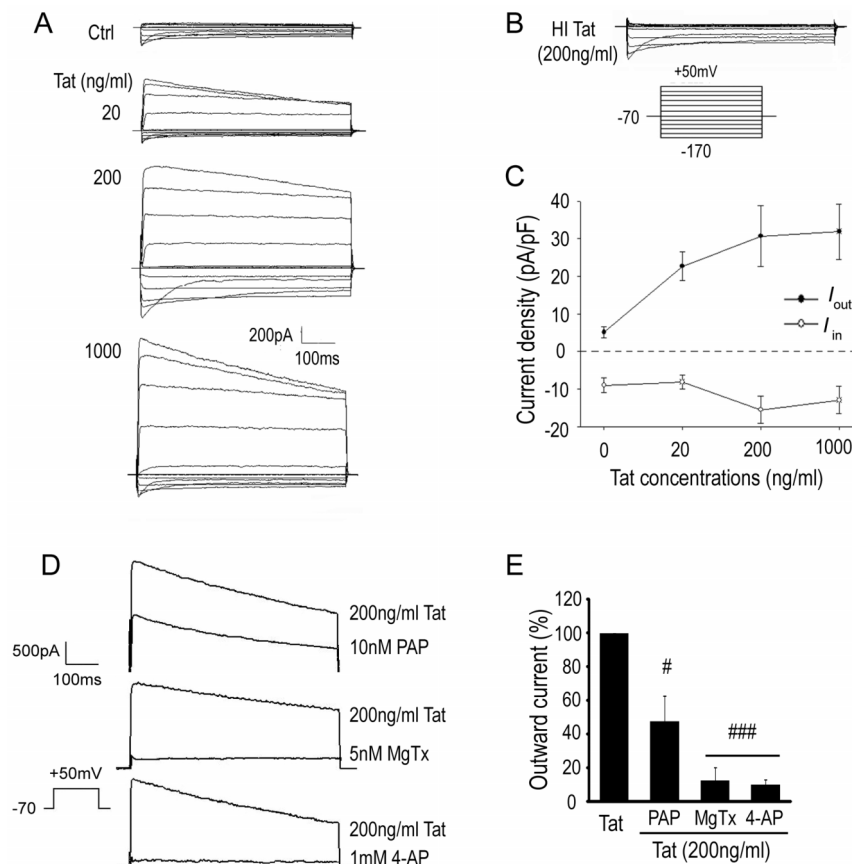


**Figure 1. HIV-1 Tat protein enhances outward K<sup>+</sup> currents ( $I_{out}$ ) in rat microglia.** **A:** Representative whole-cell membrane currents recorded from microglia treated with or without Tat at varied concentrations (0, 20, 200, 1000 ng/ml). **B:** Whole-cell membrane current recordings of microglia treated with heat-inactivated Tat (200 ng/ml). **C:** Dose-response curve of the Tat-induced effect on  $I_{out}$ . Current densities in response to different concentrations of Tat is calculated (mean  $\pm$  S.E.M) from 32, 25, 27 and 24 different cells in control, 20 ng/ml, 200 ng/ml, 1000 ng/ml groups. **D:** Pharmacology of Tat-induced  $I_{out}$ . Tat induced  $I_{out}$  were evoked by voltage from the holding potential  $-70$  mV to  $+50$  mV for 600 ms are shown before and during superfusion with extracellular solution containing 10 nM PAP, 5 nM MgTX, 1 mM 4-AP. **E:** Blockade of Tat(200 ng/ml) enhancement of  $I_{out}$  by specific Kv1.3 blockers PAP (n = 8) and MgTx (n = 8) or by a broad spectrum K<sup>+</sup> channel blocker 4-AP (n = 7). #  $p < 0.05$  vs Tat; ###  $p < 0.001$  vs Tat. doi:10.1371/journal.pone.0064904.g001

compared to  $(0.42 \pm 0.16$  nM) in untreated matched controls (Fig. 4C). This production was significantly limited ( $p < .01$ ) by blockade of K<sub>v</sub> channels using either MgTx ( $15.81 \pm 0.56$  nM), PAP ( $11.00 \pm 3.20$  nM), or 4-AP ( $16.96 \pm 1.60$  nM). Similarly, ROS production in Tat-stimulated microglia was found to be  $590.64 \pm 160.72\%$  of the level in untreated control (Fig. 4D). Pretreatment with MgTx, PAP, or 4-AP prior to the addition of Tat significantly reduced the levels of ROS to  $175.76 \pm 62.37\%$ ,  $169.91 \pm 84.58\%$ , and  $252.70 \pm 89.4\%$  of control, respectively. Collectively, these results strongly support a critical role for K<sub>v</sub>1.3 channels in the production and secretion of neurotoxins by Tat-activated microglia.

### Neurotoxic activity of Tat-stimulated microglia is mitigated by knockdown of K<sub>v</sub>1.3 gene

Having demonstrated HIV-1 Tat upregulates K<sub>v</sub>1.3 expression in rat microglia and that K<sub>v</sub>1.3 channels are involved in Tat-induced microglia-mediated neurotoxicity, complementary experiments were next performed to address whether gene silencing by knockdown of the K<sub>v</sub>1.3 gene (KCNA3) with siRNA would attenuate these effects. First, microglia were transfected with K<sub>v</sub>1.3-siRNA or nonspecific GAPDH control siRNA (control

siRNA) for 48 hr or 72 hr, depending on whether mRNA or protein expression was to be measured, and incubated with or without 200 ng/ml Tat for an additional 24 hr. RT-PCR and western blot were then used to examine K<sub>v</sub>1.3 mRNA expression and K<sub>v</sub>1.3 protein levels, respectively. As expected, the upregulation of K<sub>v</sub>1.3 mRNA expression in Tat-stimulated microglia was efficiently inhibited by transfection with K<sub>v</sub>1.3 siRNA as compared to those transfected with control siRNA (Fig. 5A). Paralleling these results, Tat-enhanced K<sub>v</sub>1.3 protein expression was found to be significantly decreased with K<sub>v</sub>1.3 siRNA transfection (Fig. 5B).

To examine the effect of K<sub>v</sub>1.3 channel knockdown on the neurotoxic properties of Tat-exposed microglia, we again employed measures of neuronal viability and apoptosis. For this experiment, microglia were transfected with K<sub>v</sub>1.3-siRNA for 72 hr and then incubated with 200 ng/ml Tat protein an additional 24 hr. Microglial supernatants were next collected and applied at 1:5 dilution to rat cortical neurons. Neurons were then incubated for an additional 24 hr before being assessed by MTT assay and TUNEL staining. As demonstrated by MTT assay, the decline in neuronal viability due to Tat-exposed microglial supernatants ( $66.87 \pm 2.55\%$ ) was improved by pre-transfection with K<sub>v</sub>1.3-siRNA ( $84.70 \pm 3.93\%$ ) (Fig. 5C). Similar-

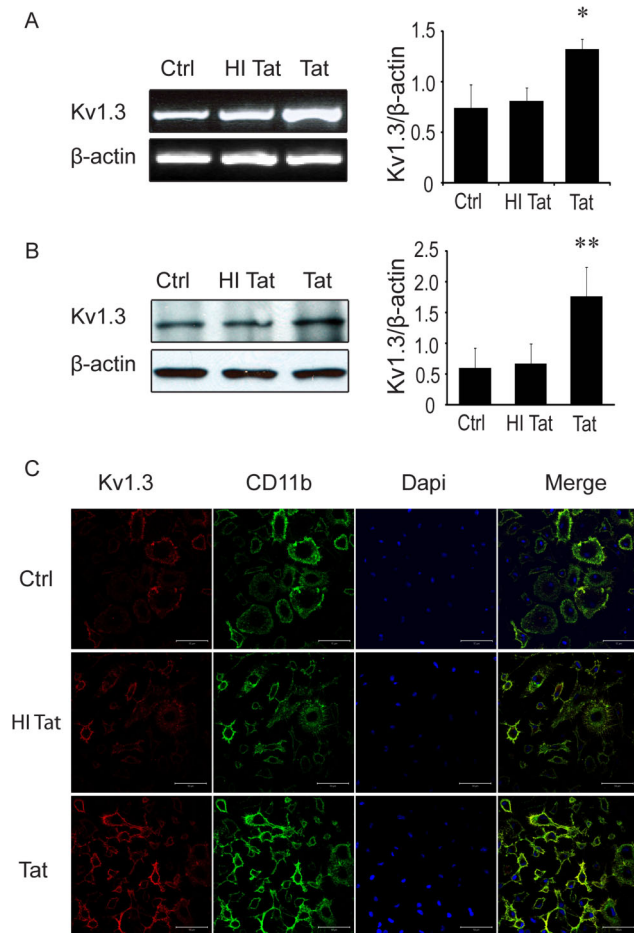


**Figure 2. Tat upregulates microglia K<sub>v</sub>1.3 channel expression.**

**A:** A representative RT-PCR gel (left) and its corresponding densitometry bar graph (right) showing enhanced levels of K<sub>v</sub>1.3 mRNA in microglia treated with Tat (200 ng/ml), but not heat-inactivated Tat (HI Tat, 200 ng/ml). **B:** The levels of K<sub>v</sub>1.3 protein was also elevated by Tat as detected by Western blot (left) and its densitometry bar graph (right). Data were obtained from three independent experiments. **C:** Tat-activated microglia were immunostained for expression of K<sub>v</sub>1.3 (red), CD11b (green) and Dapi nuclei. Images were visualized by fluorescent confocal microscopy at  $\times 400$  original magnification. Scale bars are equal to 50  $\mu$ m. \*  $p < 0.05$ , \*\*  $p < 0.01$  vs Ctrl. doi:10.1371/journal.pone.0064904.g002

ly, TUNEL staining revealed the percentage of apoptotic neurons was decreased from  $31.40 \pm 3.37\%$  to  $11.8 \pm 3.03\%$  with K<sub>v</sub>1.3 gene knockdown (Fig. 5D & 5E). The capacity for K<sub>v</sub>1.3 gene knockdown to mitigate the neuronal damage caused by Tat-activated microglia indicates the upregulation of K<sub>v</sub>1.3 mRNA and protein is a key component in the mechanism of this neurotoxicity.

#### ERK1/2 MAPK signaling pathway involvement in Tat-induced microglial neurotoxicity

Thus far we have shown Tat-induced upregulation of K<sub>v</sub>1.3 channels and currents to be critical to the activation of microglia and subsequent damage to neurons. To better clarify the mechanisms underlying these observations, we next turned our attention to the extracellular signal-related kinases (ERK1/2) MAPK signaling pathway, which has been implicated elsewhere in chronic neurodegenerative disease and may mediate the channel

profile alterations associated with Tat exposure [30,31,32]. For this experiment, microglia were exposed to 200 ng/ml Tat and proteins were harvested at various time points for assessment by western blot. Our results demonstrate ERK1/2 phosphorylation (pERK1/2) was enhanced by Tat exposure beginning at 30 min and peaking at 5 hr after stimulation (Fig. 6A). To determine if ERK1/2 activation mediates the Tat-induced increases in K<sub>v</sub>1.3 channel expression and subsequent neurotoxicity, U0126 was used to inhibit MEK1 and MEK2, the MAPK kinases responsible for phosphorylation of ERK1/2 MAPK. Reduction of ERK1/2 MAPK activity using U0126 (10  $\mu$ M) was found to markedly reduce both the expression levels of microglial K<sub>v</sub>1.3 (Fig. 6C) and the neurotoxicity of supernatants collected from Tat-exposed microglia (Fig. 6D). These results provide evidence for the involvement of the ERK MAPK pathway in Tat-induced K<sub>v</sub>1.3 expression and consequent microglia neurotoxic activity. Lastly and perhaps surprisingly, application of MgTx (5 nM), PAP (10 nM), or 4-AP (1 mM) to microglia after 30 min of Tat exposure was also found to significantly inhibit the Tat-enhanced phosphorylation of ERK1/2 (Fig. 6B).

#### K<sub>v</sub>1.3 channel involvement in ex vivo HIV-1 Tat-induced microglia-mediated neurotoxicity

Thus far we have demonstrated Tat protein exposure results in the upregulation of K<sub>v</sub>1.3 expression and the production of neurotoxic substances in cultured microglia. To better approximate *in vivo* conditions, we next used a rat hippocampal slice culture to evaluate *ex vivo* the alterations in microglial K<sub>v</sub>1.3 expression and neuronal apoptosis resulting from HIV-1 Tat application. Hippocampal slices were first dissected from rats aged 20–30 days, cultured in NeuroBasal medium, and incubated for 24 hr with 200 ng/ml Tat protein. Brain slices were then double stained with the microglia marker Iba1 and K<sub>v</sub>1.3 antibodies. In Tat protein treated slices, K<sub>v</sub>1.3 expression was found to be enhanced and co-localized with Iba1 stained microglia (Fig. 7A). In addition, TUNEL staining revealed Tat-induced neuronal apoptosis could be attenuated with 30 min K<sub>v</sub> channel antagonist pre-treatment, either MgTx (5 nM), PAP (10 nM), or 4-AP (1 mM) (Fig. 7B). These results are fully consistent with our *in vitro* studies and corroborate the involvement of K<sub>v</sub>1.3 channels in the neuronal damage caused by Tat-activated microglia.

#### Discussion

Microglia are functionally related to cells of the monocyte/macrophage lineage and play an important role as resident immunocompetent phagocytic cells in the HAND pathogenesis. A prominent pathological feature in HIV-1-infected brain is microglia activation and the activated microglia exert neurotoxic effects in the brain by releasing a variety of potentially neurotoxic substances. In addition to their production of neurotoxins, microglia express a large number of chemokine receptors that are involved in cell migration and serve as co-receptors for HIV-1 infection. Indeed, microglia are the predominant resident CNS cell type productively infected by HIV-1 [8,9]. Due to poor penetration of antiretroviral drugs through the blood-brain barrier (BBB), resident microglia (and brain macrophages) constitute a cellular reservoir of HIV-1 in the brain and a source of potential neurotoxic substances [33,34,35]. Thus, suppression of microglia production of neurotoxins is critical to the control of HAND onset and progression. In the present study, we demonstrated HIV-1 Tat-induced microglia activation and associated neurotoxicity requires K<sub>v</sub>1.3 channel activity. Exposure of microglia to HIV-1 Tat protein was found to enhance both K<sub>v</sub>1.3 currents and

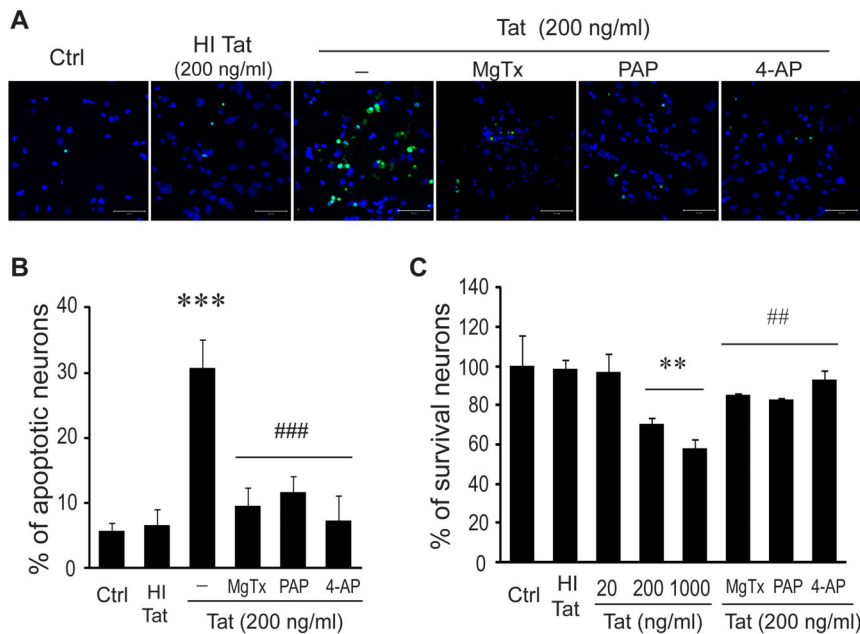


**Figure 3. K<sub>v</sub> channel antagonists attenuate Tat-induced microglia neurotoxicity.** Neurons were exposed to conditioned media recovered from microglia pre-treated with MgTx (5 nM), PAP (10 nM), or 4-AP (1 mM) for 30 min followed by Tat at varied concentrations (0, 20, 200, 1000 ng/ml). After 24 hr treatment, TUNEL staining and MTT were performed. **A:** TUNEL positive neurons were visualized by confocal microscopy at  $\times 400$  original magnification. Scale bar equals 50  $\mu$ m. Note that Tat-treated conditioned media, but not heat inactivated Tat (HI Tat)-treated conditioned media, induced neuronal apoptosis and that the Tat-induced neuronal apoptosis was blocked by MgTx, PAP or 4-AP. **B:** Quantitative exhibition of apoptotic neurons determined by ratio of the number of TUNEL-positive cells to the total number of Dapi-positive cells under different experimental conditions as indicated. **C:** MTT assay showed increased viabilities in MgTx, PAP, and 4-AP-treated groups, respectively. Data were from three independent experiments. \*\*  $p < 0.01$ , \*\*\*  $p < 0.001$  vs Ctrl; ##  $p < 0.01$ , ###  $p < 0.001$  vs conditioned media treated with Tat alone. doi:10.1371/journal.pone.0064904.g003

production of neurotoxins including IL-1 $\beta$ , TNF- $\alpha$ , NO and ROS, ultimately leading to neuronal damage. Suppression of K<sub>v</sub>1.3 channels, either by K<sub>v</sub>1.3 channel antagonists or via gene knockdown, significantly inhibited Tat-induced microglia-mediated neurotoxicity. These findings indicate K<sub>v</sub>1.3 channel modulation has the potential to mitigate microglia-associated neurotoxic activity.

Microglia express a defined pattern of K<sub>v</sub> channels including inward rectifier K<sub>ir</sub>2.1 and outward rectifiers K<sub>v</sub>1.5 and K<sub>v</sub>1.3 [19,36]. Exposure to a variety of stimuli produces a characteristic pattern of up-regulation of K<sub>v</sub>1.3 and activation of microglia results in neuronal injury via a process requiring K<sub>v</sub>1.3 activity [13,14,15,16]. In a previous study we found HIV-1 gp120 exposure activates microglia, in conjunction with enhanced K<sub>v</sub>1.3 expression and outward K<sup>+</sup> currents, leading to neuronal apoptosis [24,25]. The gp120-induced microglial neurotoxicity was significantly attenuated via suppression of K<sub>v</sub>1.3 expression or blockade of K<sub>v</sub>1.3 current. Similarly, our present study revealed exposure to HIV-1 Tat increases microglial K<sub>v</sub>1.3 channel expression and outward K<sup>+</sup> current in association with activation, neurotoxin secretion, and neuronal apoptosis, which were successfully inhibited by either siRNA knockdown of the K<sub>v</sub>1.3 gene (Fig. 4) or specific K<sub>v</sub>1.3 blockers MgTx and PAP (Fig. 1, Fig. 2, and Fig. 7). We confirmed these results in an *ex vivo* study using hippocampal slice culture, in which HIV-1 Tat-induced microglia-mediated neuronal apoptosis was attenuated by pre-treatment with K<sub>v</sub>1.3 antagonists MgTx or PAP, or a broad spectrum K<sub>v</sub> channel blocker, 4-AP. Collectively, these findings reveal the integral role of K<sub>v</sub>1.3 channels in regulating microglia activation and establish a new approach for controlling microglia mediated neurotoxic activity.

Although reported in several studies to be associated with diseases including B cell lymphoma [37], breast cancer [38,39] and Alzheimer's disease [40], research on the importance of enhanced microglial K<sub>v</sub>1.3 channel activity in HIV-1 related cognitive impairment has thus far been sparse. The evidence for the pivotal role of microglia in HAND pathogenesis is abundant however, as microglia are well known to mediate HIV entry into the brain, serve as a reservoir for productive and latent HIV-1 infection, and function as a source of neurotoxic substances [8,19,41,42,43]. After infection with HIV-1, microglia undergo dramatic phenotypic, immunological, and functional changes to produce the cytokines, chemokines, superoxides, and viral proteins that result in neuronal injury. In order to determine the role of microglial K<sub>v</sub>1.3 in this process, we examined the neurotoxic secretions of HIV-1 Tat-treated microglia in relation to K<sub>v</sub>1.3 channel activity. We found blockade of K<sub>v</sub>1.3 channels using either specific K<sub>v</sub>1.3 antagonists, MgTx and PAP, or a broad spectrum K<sub>v</sub> blocker, 4-AP, was sufficient to inhibit microglial production of IL-1 $\beta$ , TNF- $\alpha$ , NO, and ROS. These results are consistent with our previous findings [24] and suggest enhanced microglial K<sub>v</sub>1.3 channel activity is required for the HIV-1 Tat-induced secretion of neurotoxins by microglia.

HIV-1 Tat exposure has been shown to lead to microglia/macrophage activation, neurotoxin secretion, and subsequent neuronal damage [22,44,45,46] in a process mediated through microglial signal transduction pathways such as ERK1/2, PI3K, and p38 MAPK [47,48]. Tat protein has also been shown capable of increasing an outward-rectifying K<sup>+</sup> current in rat microglia through regulation of transcription factor NF- $\kappa$ B [49]. However, while K<sub>v</sub>1.3 channel activity has here been demonstrated to be necessary for Tat-induced microglial neurotoxicity, the underlying



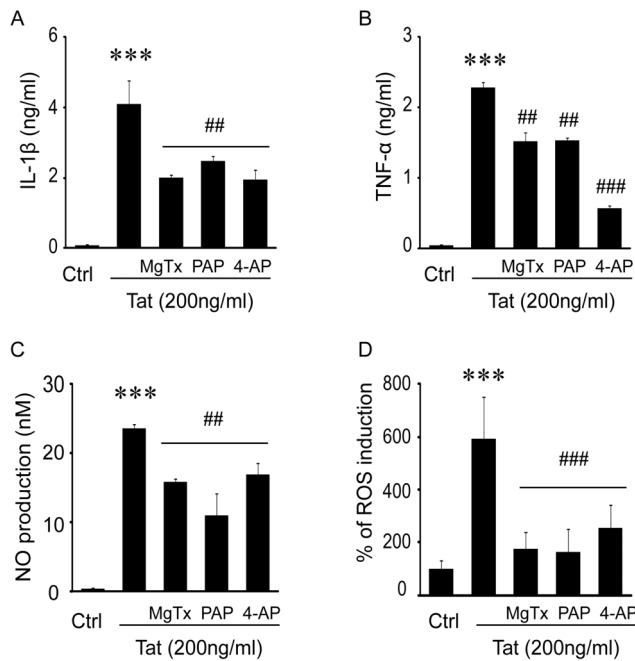


**Figure 4. K<sub>v</sub> channel blockers inhibited Tat-activated microglia secretion of neurotoxins.** Microglia were treated with MgTx (5 nM), PAP (10 nM), or 4-AP (1 mM) for 30 min before addition of Tat at 200 ng/ml. After 24 hr incubation, the supernatants were harvested for detection of IL-1 $\beta$  (A), TNF- $\alpha$  (B), NO (C) and the cells were used for analysis of ROS production (D). Data presented were from three independent experiments. \*\*\*  $p < 0.001$  vs Ctrl; ##  $p < 0.01$  or ###  $p < 0.001$  illustrates Tat alone vs pre-Tat plus MgTx, PAP or 4-AP. doi:10.1371/journal.pone.0064904.g004

connection remains to be elucidated. Although the breadth of mechanisms for modulating K<sub>v</sub> channels are numerous, including regulation of gene expression, post-translational modification, direct interactions with organic molecules and peptides, and responsiveness to membrane potential, to name a few, we chose as an appropriate starting place those signaling pathways which can convert an extracellular signal such as HIV-1 Tat protein into a functional cellular response. In particular, we focused on ERK1/2, which constitute one of the MAPK pathways that commonly transduce microenvironmental conditions in microglia and have been implicated in chronic neurodegenerative diseases [30,31,32]. Depending on the cell type, the stimulus, and the duration of cell activation, a variety of biological responses including cell proliferation, differentiation, migration, and apoptosis have been correlated with ERK activation [30,31,32]. In the present study, we explored whether ERK1/2 activation was involved in the enhancement of microglial K<sub>v</sub>1.3 expression and neuronal apoptosis resulting from exposure to HIV-1 Tat. We found ERK1/2 phosphorylation increased in HIV-1 Tat-treated microglia in a time-dependent manner (Fig. 6A), but could be prevented by pre-treatment with U1026, an inhibitor of the upstream kinase responsible for regulating ERK1/2 activity. Furthermore, pre-treatment with U1026 ameliorated Tat-induced microglial K<sub>v</sub>1.3 expression and associated neurotoxicity (Fig. 6C, Fig. 6D), indicating this process is dependent on activation of the ERK1/2 MAPK pathway. Lastly, our experiments revealed the novel finding that HIV-1 Tat-induced ERK1/2 phosphorylation could be inhibited with K<sub>v</sub> channel antagonists, MgTx, PAP, or 4-AP. It appears that while Tat-induced microglial K<sub>v</sub>1.3 expression is dependent on ERK1/2 MAPK, this same pathway is also

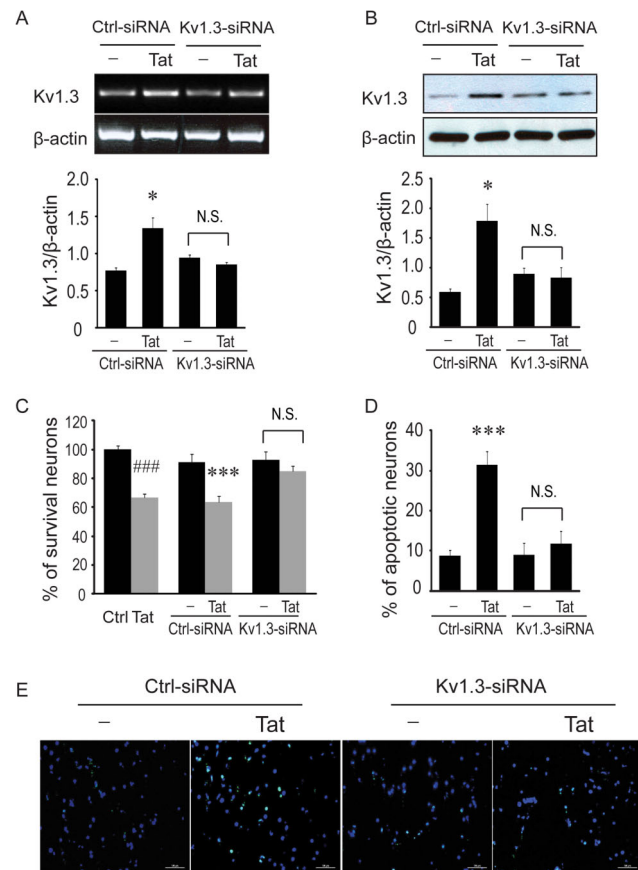


**Figure 5. K<sub>v</sub>1.3 siRNA abrogates neurotoxic activity of Tat-activated microglia.** Microglia were transfected with siRNA targeting K<sub>v</sub>1.3 (K<sub>v</sub>1.3-siRNA) or nonspecific GAPD control siRNA (Ctrl-siRNA) for 48 or 72 hr, followed by an additional 24 hr exposure to Tat (200 ng/ml). Cells were then harvested for detections of K<sub>v</sub>1.3 mRNA (48 hr post-transfection/24 hr Tat treatment) and K<sub>v</sub>1.3 proteins (72 hr post-transfection/24 hr Tat treatment). Supernatants were subjected to neuronal culture. Neuronal apoptosis and viability assay were determined using TUNEL staining and MTT assay. **A:** Representative gels show RT-PCR products for K<sub>v</sub>1.3 mRNA and internal control β-actin and bar graph reflects the density of each band after normalization of its β-actin. **B:** Western blots show K<sub>v</sub>1.3 protein and internal control β-actin protein expression of microglia, and bar graph shows densitometric quantification of each band. **C:** Collected supernatants were subjected to primary neuronal culture at a dilution of 1:5 for 24 hr and neuronal viability was evaluated by MTT assay. An increased viability was observed in neurons treated with supernatants recovered from microglia transfected with K<sub>v</sub>1.3-siRNA, but not transfected with Ctrl-siRNA. **D:** Transfection of microglia with K<sub>v</sub>1.3-siRNA significantly reduced neuronal apoptosis. In contrast, transfection of microglia with Ctrl-siRNA exhibited no significant protective effect. **E:** Apoptotic neurons were visualized by fluorescence microscopy at ×400 original magnification. Scale bar equals 100 μm. \*  $p < 0.05$ , \*\*\*  $p < 0.001$  vs Ctrl-siRNA; ###  $p < 0.001$  vs Ctrl (blank). doi:10.1371/journal.pone.0064904.g005

responsive to K<sub>v</sub> currents. Given that K<sub>v</sub> currents set the membrane potential and thus influence Ca<sup>2+</sup> influx, the latter effect may be mediated through Ca<sup>2+</sup>-dependent intracellular processes or pathways. While more investigation is necessary, this reciprocal regulation may allow for intervention in the crucial transition between functional immune activation and reactive microgliosis.

In this study, we provided evidence demonstrating K<sub>v</sub>1.3 channels to be an integral component of HIV-1 Tat-induced



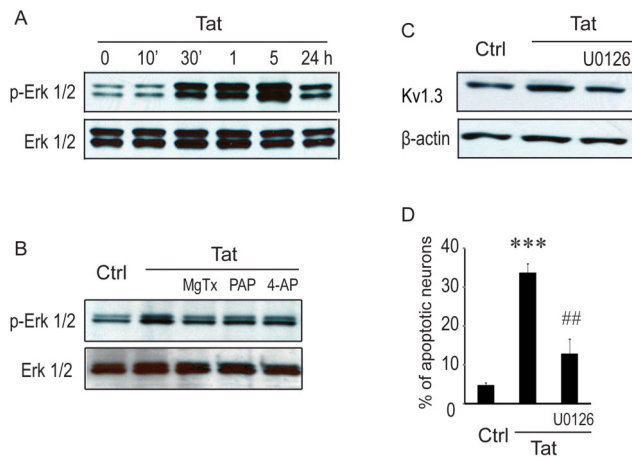


**Figure 6. Involvement of ERK1/2 MAPK pathway in Tat-mediated upregulation of Kv1.3 expression.** **A:** Western blot analysis for ERK1/2 MAPK. Microglia were exposed to 200 ng/ml of Tat and harvested at indicated times. Protein expression was analyzed by immunoblot using antibodies against ERK1/2 phosphorylation (pERK1/2) and total ERK1/2 (ERK1/2) MAPK. Tat up-regulated pERK1/2 MAPK in a time window from 30 min to 5 hr. **B:** K<sub>v</sub> channel antagonists inhibit ERK1/2 MAPK phosphorylation. Microglia were treated with MgTx (5 nM), PAP (10 nM), or 4-AP (1 mM) for 30 min followed by Tat at 200 ng/ml for additional 5 hr. Gel blots reveal a reduction of Tat-induced ERK1/2 phosphorylation in microglia treated with MgTx, PAP, or 4-AP, indicating a link between K<sub>v</sub> 1.3 channel activation and ERK1/2 MAPK signal pathway. **C:** Western blot results showing that the blockade of Tat enhancement of K<sub>v</sub>1.3 expression in microglia was blocked by U0126, an inhibitor for MEK1 and MEK 2, further demonstrating the link between ERK1/2 MAPK and Tat-induced increase of K<sub>v</sub>1.3 expression. **D:** TUNEL staining exhibited a significant increase of neuronal apoptosis induced by the supernatants collected from Tat-treated microglia and its blockade by U0126, a MEK1 and MEK2 inhibitor. Data were from three independent experiments. \*\*\*  $p < 0.001$  vs Ctrl; ##  $p < 0.001$  vs Tat-treated alone. doi:10.1371/journal.pone.0064904.g006

microglia-mediated neurotoxicity and a potential site of regulation. This promising data opens the future possibility of using K<sub>v</sub>1.3 channel inhibitors as a novel strategy to combat HAND and other neurodegenerative disorders in which the pathophysiological process involves microglia-mediated immune and inflammatory responses. In a previous *in vivo* study, we demonstrated the administration of K<sub>v</sub> channel antagonist 4-AP could ameliorate HIV-1-induced encephalitis and cognitive disorder, improving spatial learning and memory in a severe combined immunodeficient (SCID) mouse model of HIV-1 encephalitis (HIVE) [50]. Nevertheless, as K<sub>v</sub> channel blockers selectively target immune cells including macrophage, microglia, and lymphocytes, the therapeutic benefit of this approach must be carefully considered for potential risks to the immune system. Of these cells, the most abundant K<sub>v</sub>1.3 channel expression is reported to be found the human effector memory T cells (CD4<sup>+</sup>CCR7<sup>-</sup>CD45RA<sup>+</sup>), which regulate Th1 cell inflammatory responses [36,51,52]. The use of small molecule K<sub>v</sub> blockers, such as verapamil, diltiazem, and nifedipine, has been shown to reduce IL-12 secretion and inhibit T cell proliferation [53]. Notably, these immunomodulatory effects have been found to depend heavily on the level of K<sub>v</sub>1.3 channel expression, which changes dramatically as T cells differentiate from naïve to memory states or transition from resting to activation [54,55,56]. Given that the immune response functions of microglia, macrophage, Helper T cells, and B cells remain

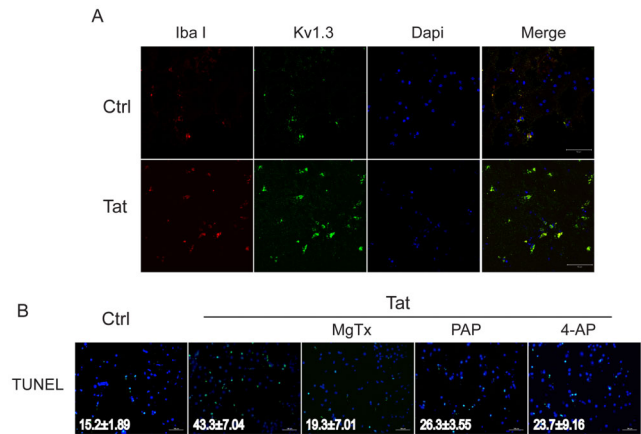


**Figure 7. K<sub>v</sub> channel blockers ameliorated Tat-induced microglia neurotoxicity in rat hippocampus slices.** Rat hippocampus slices were pretreated with MgTx (5 nM), PAP (10 nM), or 4-AP (1 mM) for 30 min before addition of Tat (200 ng/ml). Immunohistochemistry or TUNEL staining was performed 24 hr later. **A:** Tat increased levels of K<sub>v</sub>1.3 expression that were co-localized with microglia (Iba1 staining) in rat hippocampus slices. Rat hippocampus slices were stained with mouse anti-Iba1 Ab (1:1000, red), whereas K<sub>v</sub>1.3 was stained with goat polyclonal antibody (1:200, green). Images were visualized by confocal microscopy. **B:** TUNEL staining showed that Tat produced neuronal apoptosis in rat hippocampus slices that was attenuated by MgTx, PAP, or 4-AP. Numerical numbers in each image panel represents the average apoptotic cells (M ± SD, n = 3 slices, 5 random visual fields were counted in each slice) in experimental conditions as indicated. doi:10.1371/journal.pone.0064904.g007

basically intact, the potential side effects of pharmacologically blocking K<sub>v</sub>1.3 channels could be minimal [52,57]. In fact, the potential side effects of using K<sub>v</sub> channel blockers to treat a wide range of autoimmune conditions, including those involving effector memory T cells, delayed type hypersensitivity, type 1 diabetes, rheumatoid arthritis, multiple sclerosis, and inflammatory bone resorption, have been investigated without revealing any generalized immunosuppression [58,59,60,61]. Recently, the safety of this approach was given further credence when the US Food and Drug Administration approved the K<sub>v</sub> channel blocker dalfampridine (Ampyra) as a treatment multiple sclerosis (<http://www.fda.gov/NewsEvents/Newsroom/PressAnnouncements/ucm198463.htm>).

In summary, the present study serves to establish the integral role of K<sub>v</sub>1.3 channel activity in HIV-1 Tat-induced microglia-mediated neurotoxicity. The identification of K<sub>v</sub>1.3 channels as a point of intervention in this process may open new avenues for therapeutic modalities. Given its feasibility and safety, it may now be advantageous to consider studying a K<sub>v</sub>1.3 channel-based therapeutic approach in the treatment of HAND and other neurodegenerative disorders characterized by microglia-mediated neuroinflammation.

## Acknowledgments

The Authors thank Ms. Julie Ditter, Ms. Robin Taylor, Ms. Johna Belling and Ms. Sandra Wiese for their excellent administrative support.

## Author Contributions

Conceived and designed the experiments: JL HX. Performed the experiments: JL PX CC HL JZ. Analyzed the data: JL PX CC HX. Wrote the paper: JL JK HX.

## References

- Kaul M, Lipton SA (2006) Mechanisms of neuronal injury and death in HIV-1 associated dementia. *Curr HIV Res* 4: 307–318.
- Antinori A, Arendt G, Becker JT, Brew BJ, Byrd DA, et al. (2007) Updated research nomenclature for HIV-associated neurocognitive disorders. *Neurology* 69: 1789–1799.
- Robertson KR, Smurzynski M, Parsons TD, Wu K, Bosch RJ, et al. (2007) The prevalence and incidence of neurocognitive impairment in the HAART era. *AIDS* 21: 1915–1921.
- Heaton RK, Clifford DB, Franklin DR Jr, Woods SP, Ake C, et al. (2010) HIV-associated neurocognitive disorders persist in the era of potent antiretroviral therapy: CHARTER Study. *Neurology* 75: 2087–2096.
- Spudis SS, Ances BM (2011) Central nervous system complications of HIV infection. *Top Antivir Med* 19: 48–57.
- Glass JD, Fedor H, Wesselingh SL, McArthur JC (1995) Immunocytochemical quantitation of human immunodeficiency virus in the brain: correlations with dementia. *Ann Neurol* 38: 755–762.
- Gendelman HE, Eiden L, Epstein L, Grant I, Lipton S, et al. (1998) The Neuropathogenesis of HIV-1-Dementia: APANEL Discussion. In: Gendelman HE, Lipton SA, Epstein LG, Swindells S, editors. *The neurology of AIDS*. 1 ed. New York: Chapman and Hall. pp. 1–10.
- Garden GA (2002) Microglia in human immunodeficiency virus-associated neurodegeneration. *Glia* 40: 240–251.
- Kielian T (2004) Microglia and chemokines in infectious diseases of the nervous system: views and reviews. *Front Biosci* 9: 732–750.
- Kettenmann H, Hanisch UK, Noda M, Verkhratsky A (2011) Physiology of microglia. *Physiol Rev* 91: 461–553.
- Wickenden A (2002) K<sup>+</sup> channels as therapeutic drug targets. *Pharmacol Ther* 94: 157–182.
- Judge SI, Lee JM, Bever CT Jr, Hoffman PM (2006) Voltage-gated potassium channels in multiple sclerosis: Overview and new implications for treatment of central nervous system inflammation and degeneration. *J Rehabil Res Dev* 43: 111–122.
- Norenberg W, Gebicke-Haerter PJ, Illes P (1994) Voltage-dependent potassium channels in activated rat microglia. *J Physiol* 475: 15–32.
- Fischer HG, Eder C, Hadding U, Heinemann U (1995) Cytokine-dependent K<sup>+</sup> channel profile of microglia at immunologically defined functional states. *Neuroscience* 64: 183–191.
- Eder C (1998) Ion channels in microglia (brain macrophages). *Am J Physiol* 275: C327–342.
- Schilling T, Quandt FN, Cherny VV, Zhou W, Heinemann U, et al. (2000) Upregulation of Kv1.3 K<sup>+</sup> channels in microglia deactivated by TGF- $\beta$ . *Am J Physiol Cell Physiol* 279: C1123–1134.
- Kettenmann H, Hoppe D, Gottmann K, Banati R, Kreutzberg G (1990) Cultured microglial cells have a distinct pattern of membrane channels different from peritoneal macrophages. *J Neurosci Res* 26: 278–287.
- Eder C, Schilling T, Heinemann U, Haas D, Hailer N, et al. (1999) Morphological, immunophenotypical and electrophysiological properties of resting microglia in vitro. *Eur J Neurosci* 11: 4251–4261.
- Walz W, Bekar LK (2001) Ion channels in cultured microglia. *Microsc Res Tech* 54: 26–33.
- Farber K, Kettenmann H (2005) Physiology of microglial cells. *Brain Res Brain Res Rev* 48: 133–143.
- Gendelman HE, Ding S, Gong N, Liu J, Ramirez SH, et al. (2009) Monocyte chemotactic protein-1 regulates voltage-gated K<sup>+</sup> channels and macrophage transmigration. *J Neuroimmune Pharmacol* 4: 47–59.
- Fordyce CB, Jagasia R, Zhu X, Schlichter LC (2005) Microglia Kv1.3 channels contribute to their ability to kill neurons. *J Neurosci* 25: 7139–7149.
- Nuttle-McMenemy N, Effenbein A, Delco JA (2007) Minocycline decreases in vitro microglial motility,  $\beta$ -actin-integrin, and Kv1.3 channel expression. *J Neurochem* 103: 2035–2046.
- Liu J, Xu C, Chen L, Xu P, Xiong H (2012) Involvement of Kv1.3 and p38 MAPK signaling in HIV-1 glycoprotein 120-induced microglia neurotoxicity. *Cell Death Dis* 3: e254.
- Xu C, Liu J, Chen L, Liang S, Fujii N, et al. (2011) HIV-1 gp120 enhances outward potassium current via CXCR4 and cAMP-dependent protein kinase A signaling in cultured rat microglia. *Glia* 59: 997–1007.
- Westendorp MO, Frank R, Ochsenbauer C, Stricker K, Dhein J, et al. (1995) Sensitization of T cells to CD95-mediated apoptosis by HIV-1 Tat and gp120. *Nature* 375: 497–500.
- Xiao H, Neuveut C, Tiffany HL, Benkirane M, Rich EA, et al. (2000) Selective CXCR4 antagonism by Tat: implications for in vivo expansion of coreceptor use by HIV-1. *Proc Natl Acad Sci U S A* 97: 11466–11471.
- Bonavia R, Bajetto A, Barbero S, Albini A, Noonan DM, et al. (2001) HIV-1 Tat causes apoptotic death and calcium homeostasis alterations in rat neurons. *Biochem Biophys Res Commun* 288: 301–308.
- Hayashi K, Pu H, Andras IE, Eum SY, Yamauchi A, et al. (2006) HIV-TAT protein upregulates expression of multidrug resistance protein 1 in the blood-brain barrier. *J Cereb Blood Flow Metab* 26: 1052–1065.
- Koistinaho M, Koistinaho J (2002) Role of p38 and p44/42 mitogen-activated protein kinases in microglia. *Glia* 40: 175–183.
- Strniskova M, Barancik M, Ravingerova T (2002) Mitogen-activated protein kinases and their role in regulation of cellular processes. *Gen Physiol Biophys* 21: 231–255.
- Kaminska B, Gozdz A, Zawadzka M, Ellert-Miklaszewska A, Lipko M (2009) MAPK signal transduction underlying brain inflammation and gliosis as therapeutic target. *Anat Rec (Hoboken)* 292: 1902–1913.
- Koenig S, Gendelman HE, Orenstein JM, Dal Canto MC, Pezeshtpour GH, et al. (1986) Detection of AIDS virus in macrophages in brain tissue from AIDS patients with encephalopathy. *Science* 233: 1089–1093.
- Genis P, Jett M, Bernton EW, Boyle T, Gelbard HA, et al. (1992) Cytokines and arachidonic metabolites produced during human immunodeficiency virus (HIV)-infected macrophage-astroglia interactions: implications for the neuropathogenesis of HIV disease. *J Exp Med* 176: 1703–1718.
- Kaul M, Garden GA, Lipton SA (2001) Pathways to neuronal injury and apoptosis in HIV-associated dementia. *Nature* 410: 988–994.
- Menteyne A, Levavasseur F, Audinat E, Avignone E (2009) Predominant functional expression of Kv1.3 by activated microglia of the hippocampus after Status epilepticus. *PLoS One* 4: e6770.
- Alizadeh AA, Eisen MB, Davis RE, Ma C, Lossos IS, et al. (2000) Distinct types of diffuse large B-cell lymphoma identified by gene expression profiling. *Nature* 403: 503–511.
- Abdul M, Santo A, Houssein N (2003) Activity of potassium channel-blockers in breast cancer. *Anticancer Res* 23: 3347–3351.
- Brevet M, Ahidouch A, Sevestre H, Merviel P, El Hiani Y, et al. (2008) Expression of K<sup>+</sup> channels in normal and cancerous human breast. *Histol Histopathol* 23: 965–972.
- Schilling T, Eder C (2011) Amyloid-beta-induced reactive oxygen species production and priming are differentially regulated by ion channels in microglia. *J Cell Physiol* 226: 3295–3302.
- Kramer-Hammerle S, Rothenaigner I, Wolff H, Bell JE, Brack-Werner R (2005) Cells of the central nervous system as targets and reservoirs of the human immunodeficiency virus. *Virus Res* 111: 194–213.
- Hanisch UK (2002) Microglia as a source and target of cytokines. *Glia* 40: 140–155.
- Kim SU, de Vellis J (2005) Microglia in health and disease. *J Neurosci Res* 81: 302–313.
- Dheen ST, Kaur C, Ling EA (2007) Microglial activation and its implications in the brain diseases. *Curr Med Chem* 14: 1189–1197.
- Lee YB, Schrader JW, Kim SU (2000) p38 map kinase regulates TNF- $\alpha$  production in human astrocytes and microglia by multiple mechanisms. *Cytokine* 12: 874–880.
- Nagata Y, Todokoro K (1999) Requirement of activation of JNK and p38 for environmental stress-induced erythroid differentiation and apoptosis and of inhibition of ERK for apoptosis. *Blood* 94: 853–863.
- Lokensgard JR, Hu S, Hegg CC, Thayer SA, Gekker G, et al. (2001) Diazepam inhibits HIV-1 Tat-induced migration of human microglia. *J Neurovirol* 7: 481–486.
- Eugenin EA, Dyer G, Calderon TM, Berman JW (2005) HIV-1 tat protein induces a migratory phenotype in human fetal microglia by a CCL2 (MCP-1)-dependent mechanism: possible role in NeuroAIDS. *Glia* 49: 501–510.
- Visentin S, Renzi M, Levi G (2001) Altered outward-rectifying K<sup>+</sup> current reveals microglial activation induced by HIV-1 Tat protein. *Glia* 33: 181–190.
- Keblesh JP, Dou H, Gendelman HE, Xiong H (2009) 4-Aminopyridine improves spatial memory in a murine model of HIV-1 encephalitis. *J Neuroimmune Pharmacol* 4: 317–327.
- Chandy KG, Wulff H, Beeton C, Pennington M, Gutman GA, et al. (2004) K<sup>+</sup> channels as targets for specific immunomodulation. *Trends Pharmacol Sci* 25: 280–289.
- Beeton C, Wulff H, Standifer NE, Azam P, Mullen KM, et al. (2006) Kv1.3 channels are a therapeutic target for T cell-mediated autoimmune diseases. *Proc Natl Acad Sci U S A* 103: 17414–17419.
- Chandy KG, DeCoursey TE, Cahalan MD, McLaughlin C, Gupta S (1984) Voltage-gated potassium channels are required for human T lymphocyte activation. *J Exp Med* 160: 369–385.
- Wulff H, Beeton C, Chandy KG (2003) Potassium channels as therapeutic targets for autoimmune disorders. *Curr Opin Drug Discov Devel* 6: 640–647.
- Beeton C, Wulff H, Singh S, Botsko S, Crossley G, et al. (2003) A novel fluorescent toxin to detect and investigate Kv1.3 channel up-regulation in chronically activated T lymphocytes. *J Biol Chem* 278: 9928–9937.
- Wulff H, Calabresi PA, Allie R, Yun S, Pennington M, et al. (2003) The voltage-gated Kv1.3 K<sup>+</sup> channel in effector memory T cells as new target for MS. *J Clin Invest* 111: 1703–1713.
- Vianna-Jorge R, Suarez-Kurtz G (2004) Potassium channels in T lymphocytes: therapeutic targets for autoimmune disorders? *BioDrugs* 18: 329–341.
- Beeton C, Pennington MW, Norton RS (2011) Analogs of the sea anemone potassium channel blocker ShK for the treatment of autoimmune diseases. *Inflamm Allergy Drug Targets* 10: 313–321.
- Valverde P, Kawai T, Taubman MA (2005) Potassium channel-blockers as therapeutic agents to interfere with bone resorption of periodontal disease. *J Dent Res* 84: 488–499.

60. Goffe B, Papp K, Gratton D, Krueger GG, Darif M, et al. (2005) An integrated analysis of thirteen trials summarizing the long-term safety of alefacept in psoriasis patients who have received up to nine courses of therapy. *Clin Ther* 27: 1912–1921.
61. Esamai F, Tenge CN, Ayuo PO, Ong'or WO, Obala A, et al. (2005) A randomized open label clinical trial to compare the efficacy and safety of intravenous quinine followed by oral malarone vs. intravenous quinine followed by oral quinine in the treatment of severe malaria. *J Trop Pediatr* 51: 17–24.